Breaking DNA strands by extreme-ultraviolet laser pulses in vacuum

Eva Nováková,[1] Luděk Vyšín,[1,2,*] Tomáš Burian,[1] Libor Juha,[1] Marie Davídková,[3] Viliam Múčka,[2] Václav Čuba,[2]
Michael E. Grisham,[4] Scott Heinbuch,[4] and Jorge J. Rocca[4]

[1]*Department of Radiation and Chemical Physics, Institute of Physics CAS, Na Slovance 2, Prague 8, 182 21, Czech Republic*
[2]*Department of Nuclear Chemistry, Faculty of Nuclear Sciences and Physical Engineering, Czech Technical University in Prague, Břehová 7,
Prague 1, 115 19, Czech Republic*
[3]*Department of Radiation Dosimetry, Institute of Nuclear Physics CAS, Na Truhlářce 39/64, Prague 8, 180 86, Czech Republic*
[4]*NSF ERC for Extreme Ultraviolet Science and Technology, Department of Electrical and Computer Engineering, Colorado State University,
Fort Collins, Colorado 80523-1373, USA*

Ionizing radiation induces a variety of DNA damages including single-strand breaks (SSBs), double-strand breaks (DSBs), abasic sites, modified sugars, and bases. Most theoretical and experimental studies have been focused on DNA strand scissions, in particular production of DNA double-strand breaks. DSBs have been proven to be a key damage at a molecular level responsible for the formation of chromosomal aberrations, leading often to cell death. We have studied the nature of DNA damage induced directly by the pulsed 46.9-nm (26.5 eV) radiation provided by an extreme ultraviolet (XUV) capillary-discharge Ne-like Ar laser (CDL). Doses up to 45 kGy were delivered with a repetition rate of 3 Hz. We studied the dependence of the yield of SSBs and DSBs of a simple model of DNA molecule (pBR322) on the CDL pulse fluence. Agarose gel electrophoresis method was used for determination of both SSB and DSB yields. The action cross sections of the single- and double-strand breaks of pBR322 plasmid DNA in solid state were determined. We observed an increase in the efficiency of strand-break induction in the supercoiled DNA as a function of laser pulse fluence. Results are compared to those acquired at synchrotron radiation facilities and other sources of extreme-ultraviolet and soft x-ray radiation.

PACS number(s): 87.14.G−

I. INTRODUCTION

The study of radiation damage to biomolecules is important for understanding the mechanisms of radiation damage to cells, tissues, and living organisms. All radiation injuries to tissues, organs, fetus, and the entire body begin at an injury to an individual cell. The primary target for radiation-induced cell damage is the DNA molecule [1]. Under the action of vacuum UV radiation, DNA undergoes excitation to the upper electronic states. The first ionization potential of several DNA constituents in vacuum is around 9 eV [2,3]. The vacuum UV absorption spectra of the dried DNA films exhibit a transition at 4.7 and $\sim$6.5 eV, which correspond to the $\pi \rightarrow \pi^*$ transition dipole moments originating from the amide group of the individual bases. Increased absorption at $\lambda < 160$ nm may arises from σ-electron excitations mainly associated with the sugar-phosphate chain, and $\pi \rightarrow \pi^*$ and $\sigma \rightarrow \sigma^*$ transitions of the bases. A prominent peak in the energy-loss function near 21.6 eV is associated with a collective resonance involving all the valence electrons [4,5]. Energy-absorbing modes (excitations, so-called superexcitations, outer- and inner-shell ionizations) affect the type and extent of DNA damage. Far-UV radiation is absorbed directly by the DNA bases resulting in electronic excitations and the formation of dimeric pyrimidine photoproducts [6,7]. VUV photoabsorption leads mainly to the dissociation of deoxyribose [8], through the damage sensitivity dependent on the base sequence and sugar-phosphate backbone chain length [9]. Damage at the deoxyribose sites may result in the strand-break formation through the preceding alteration of the deoxypentose.

Ultrasoft x rays induce radiation damage typical for ionizing radiation. Direct effect of ionizing radiation is caused by excitation or ionization of binding electrons in the sugars or in the phosphates. Indirect effect involves damage pathways where hydroxyl radicals which are produced in the track of the ionizing radiation or directly in the solvation shell attack the DNA molecule by diffusion. In the case of 26.5-eV photons a production of hydroxyl radicals follows photoionization and photoexcitation of water molecules [10]. Therefore both direct and indirect effects can lead to bond dissociation in DNA molecules and subsequent DNA strand-break formation.

One single-strand break (SSB) transforms a DNA molecule of the supercoiled form to the relaxed circular form, while one double-strand break (DSB) produced either directly or as the result of two closely spaced SSBs in the complementary strands changes either the supercoiled form or relaxed form to the linear form. Two SSBs on opposite strands have been assumed to lead to a DSB if separated by ten base pairs (bp) or less. Double-strand breaks are considered the most critical DNA lesions induced by ionizing radiation. Damage to bases leads to a variety of base alterations.

Experimental studies where samples of plasmid DNA were irradiated in vacuum with photons of energies in the 7–150-eV range provide evidence for the ability of photons with energy as low as 7 eV to induce both SSBs and DSBs [11]. The primary ionizing radiation generates low-energy secondary electrons in biological materials through photoelectric effect. These low-energy electrons are expected to induce biological effects more effectively than higher energy electrons or photons [12]. The authors [12] determined, using a monolayer DNA sample irradiated under vacuum conditions with extremely low-energy electrons (below 20 eV), that dissociative electron attachment

————
*vysin@fzu.cz

plays an important role in DNA strand breakage and in the decomposition of nucleobases.

Up to now, not many extended studies on XUV photon interaction with DNA has been carried out [13,14], whereas many have been done with soft x-rays photons [15–20]. This can in part be explained by a lack of easily accessible monochromatic photon sources intense enough to induce detectable amounts of molecular damage in this energy region.

The invention of the desktop, repetitive XUV laser [21], based on a collisionally pumped transition of Ne-like Ar ions in pinching plasma column of a capillary discharge [22], makes it possible to bring XUV or soft x-ray lasers from a few large-scale facilities to many laboratory rooms. The biological effects of low-energy x rays were recently studied using single subnanosecond 1-keV x-ray pulse produced by a large-scale, double-stream gas puff target, illuminated by sub-kJ, near-infrared (NIR) focused laser pulses [17]. The yields of SSBs and DSBs as well as the SSB-DSB ratio were in very good agreement with the results of other groups using soft x-ray tubes and synchrotron radiation, i.e., much lower dose rates. The ability of the plasma source to induce measurable radiobiological change by an action of even a single shot was demonstrated.

In this work, solid films of plasmid DNA were exposed to the XUV photons under the vacuum conditions. However, even under the conditions used, we cannot totally exclude the influence of water radicals [18]. It is assumed that most of the water is removed, leaving approximately three water molecules per nucleotide of DNA closely associated with the phosphate groups [23]. The DNA molecule in solid films adopts a double-helix conformation known as the *A* form. Under physiological conditions, the dominant form of DNA is the *B* form. At very low humidity, the *B* conformation becomes more compact, with 11 bases per turn instead of 10.5 in the *B* form. Its base pairs are tilted rather than perpendicular to the helix axis. The transition of *B* form to *A* form is a reversible process, depending on the levels of sample hydration [24].

II. MATERIAL AND METHODS

A. XUV source

The experimental setup we used for the radiobiological experiments is shown in Fig. 1(a). The samples were irradiated with the beam of a desktop size Ne-like Ar capillary discharge laser [21] operating at 46.9-nm wavelength (26.5 eV). Full details of this tabletop soft x-ray laser and
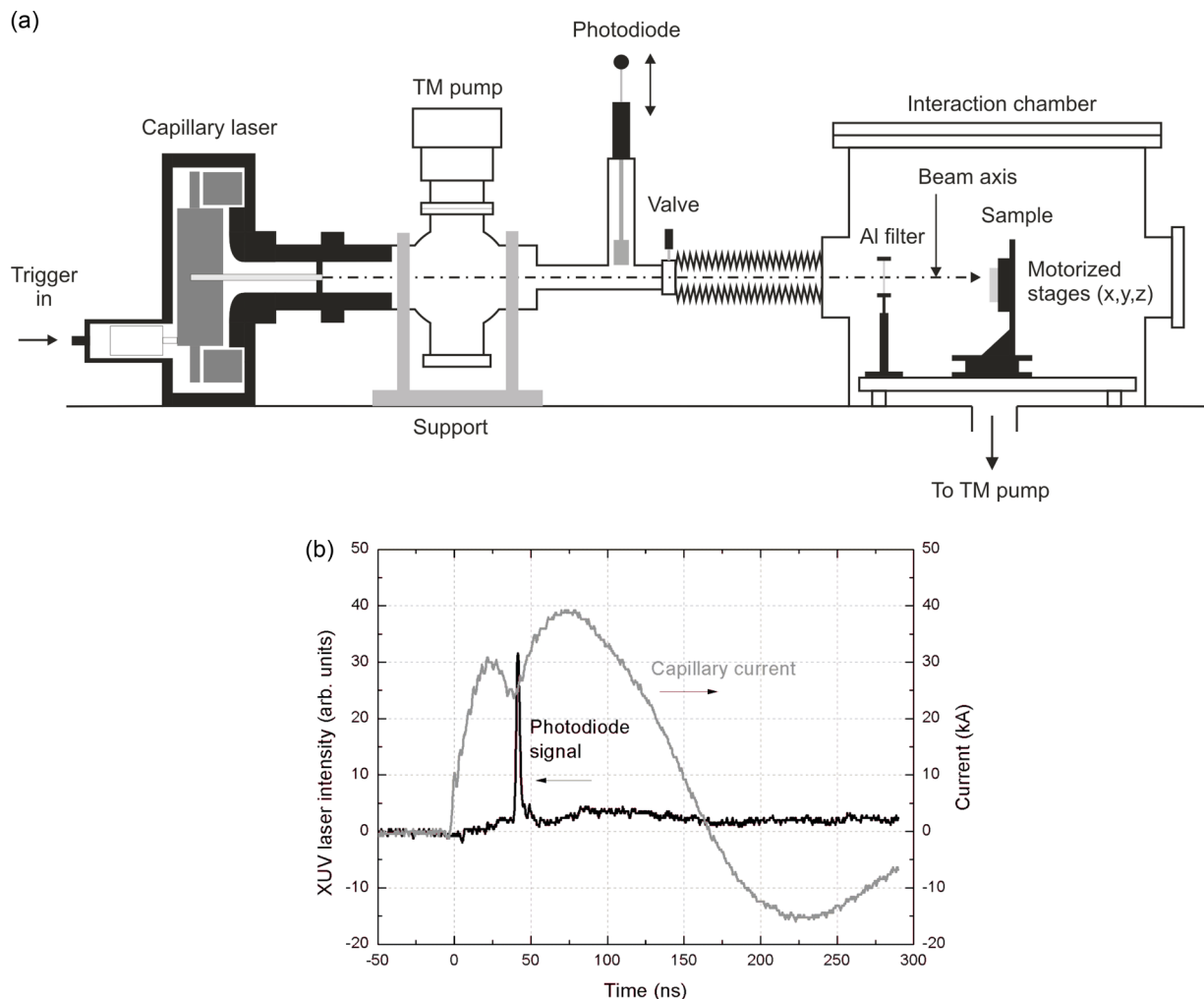
FIG. 1. (Color online) (a) Schematic layout of the capillary-discharge Ne-like Ar laser (CDL) and the vacuum chamber for irradiating plasmid DNA. (b) Time progress in discharge current and laser output intensity.
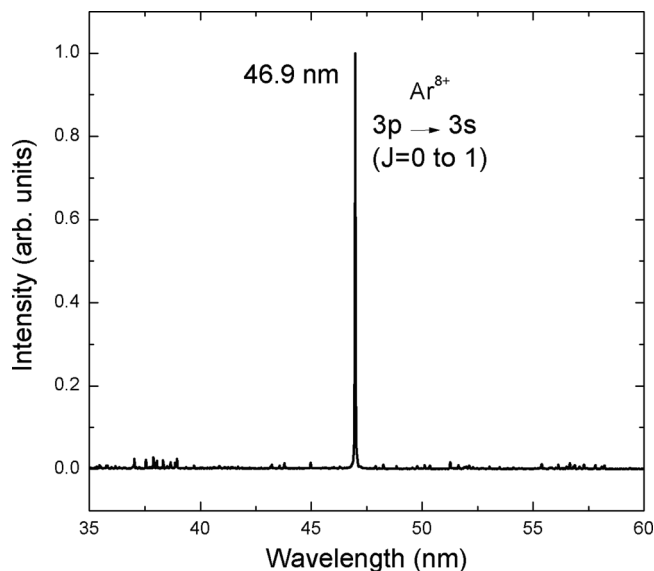
FIG. 2. XUV lasing at 46.9 nm on the $3p \to 3s$, $J = 0 \to J = 1$ transition in Ne-like argon. Axial emission spectrum (normalized at 46.9 nm) in the region between 35 and 60 nm.

vacuum interaction chamber have been given in the previous publications [21,25,26]. The discharge driven by a 22-kA peak current occurs through a 380-mTorr argon gas in a 21-cm-long and 3.2-mm-diameter capillary tube. Laser pulse energy, monitored by means of the vacuum photodiode, was adjusted to 2 μJ (5×10^{11} XUV photons/pulse) with a high shot-to-shot stability. Optimization of the plasma conditions in this device can yield up to 10-μJ pulses [21]. Measured pulse duration is of 1.5 ns full width at half maximum (FWHM) [Fig. 1(b)].

Axial emission spectrum with one dominant 46.9-nm spectral line is shown in Fig. 2. The spectrum was obtained with flat-field XUV spectrometer equipped with a back illuminated x-ray charge coupled device (CCD; Princeton Instruments) behind a 0.40-μm aluminium foil. A previous measurement of the laser linewidth showed that the emission is highly monochromatic, with $\Delta\lambda/\lambda = 3 \times 10^{-5}$ [27].

B. DNA sample preparation and manipulation

The pBR322 DNA plasmid (4361 bp) was purchased from Fermentas Life Sciences (York, UK). More than 98% of the used DNA was characterized to be in the supercoiled form. To prepare thin films of DNA, we pipetted 5 μl of solution containing 110 ng of plasmid DNA in a Tris-EDTA buffer (10 mM Tris-HCl, 1 mM EDTA, pH 7.6; abbreviated as 1X TE buffer) onto a glass coverslip (Hirschmann Laborgeräte, Eberstadt, Germany), and allowed to dry in air. The DNA samples were prepared immediately before irradiation, and redissolved in 8 μl of 1X TE buffer just after irradiation. After one dehydration-rehydration cycle, the supercoiled form of plasmid DNA decreased to about 92–95%.

After drying, a film of DNA-buffer solutes of a diameter of 3.5 ± 0.2 mm was formed on the coverslip. With a density of 1.7 g/cm^3 and a diameter of 3.5 mm, the DNA film thickness excluding buffer solute was estimated to be ∼7 nm. The thickness of DNA-buffer samples was measured by a surface

profiler (Alpha Step 500, Tencor Instruments, Mountain View, CA) to be 65–70 nm.

The thickness of the sample was chosen to secure a major role of XUV-induced radiolysis of DNA plasmid, i.e, a significant fraction of XUV photon flux is absorbed in the DNA layer not in the substrate. Thus the radiolysis by electrons emitted from the silicon substrate exposed to XUV photons passed through the DNA layer was reduced.

The fraction of XUV pulse energy deposited in the sample was estimated from the sample thickness, the density of DNA (1.7 g/cm^3), the elemental composition of pBR322 DNA (per 1 bp): C(19.4)H(24.5)N(7.5)O(12.0)P(2.0) [28,29], as well as from the density and the composition of atoms of the TE buffer solutes (1.25 g/cm^3, C(5.0)H(13.2) N(1.2)O(3.8)Na(0.3)Cl(0.6) [15]), using the photoabsorption cross-section values tabulated by Henke *et al.* [30]. We found that for our sample and 26.5-eV radiation ∼97.6% of the energy is deposited in the irradiated material (from that approximately 1.6% XUV pulse energy is directly deposited in plasmid DNA).

C. XUV irradiation

The samples were placed into the vacuum chamber at a distance of 105 cm from the source and irradiated at a repetition rate of 3 Hz. Typically, samples were irradiated when the vacuum pressure was reduced to less than 10^{-5} mbar within the sample chamber. The beam position was checked by installing a Ce:YAG scintillation crystal (Crytur Ltd., Czech Republic) at the sample position and viewing the fluorescence due to the incident radiation. We measured the laser output intensity distribution using phosphor-coated CCD array detector (PL-B781; Pixelink, Canada) of 2208×3000 pixels at the sample position. Since the sample area is smaller than the beam cross section, the fraction of the XUV laser beam hitting the sample was obtained by integrating the beam intensity distribution over the sample area.

The broadband incoherent ultraviolet-visible (UV-Vis) radiation emitted from the plasma column of the capillary discharge was filtered out using 0.15-μm- and 0.4-μm-thick aluminium foils (>17 eV, Goodfellow Cambridge Ltd, England). The effect of the broadband incoherent UV-Vis radiation exposure on plasmid DNA samples was studied by using a lithium fluoride window (<11.5 eV), filtering out 46.9-nm laser radiation.

A control sample for each series of the irradiation was placed into the vacuum chamber but was not irradiated. The remaining samples were irradiated at the same distance from the source by different number of pulses, i.e., 50–4000, screened by aluminium foils of different thicknesses.

The photon fluence in one pulse for each sample was calculated from the time progress in discharge current generated by the photodiode and corrected for the transmission of the particular aluminium foil and for the absorption in the dried buffer solute. In the experiment without use of Al foil, the photon fluence in one pulse was estimated to be ∼2×10^{15} photons/m^2, for 0.15 μm Al foil ∼0.052×10^{15} photons/m^2 and for the experiment with the use of 0.40-μm Al filter ∼0.011×10^{15} photons/m^2. In the sample with the surface density of 1.14 μg/cm^2, this corresponds to the dose of 11, 7.1, and 1.6 grays (Gy)/pulse, respectively.
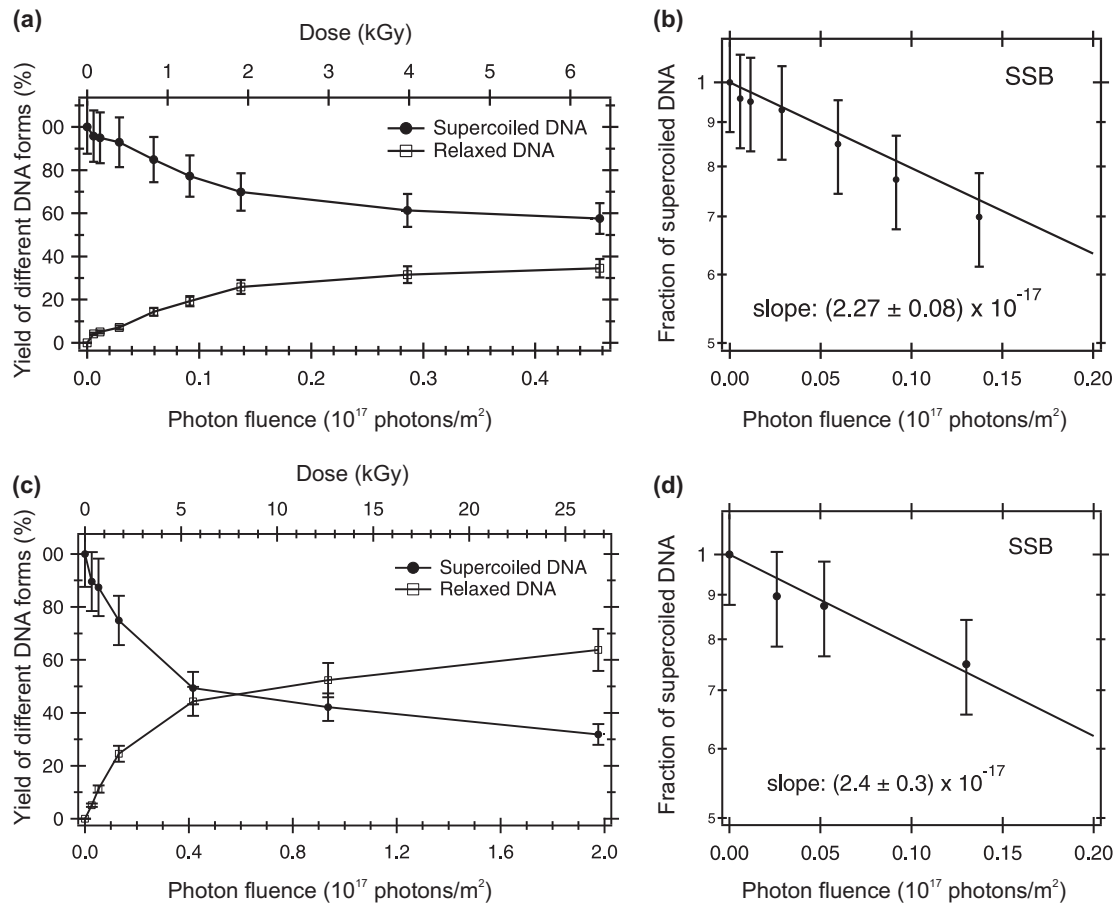
FIG. 3. Loss of supercoiled DNA and induction of SSBs in plasmid DNA as a function of photon fluence on the sample surface (the bottom axis), as well as a function of absorbed dose (the top axis), irradiated with 26.5-eV photons behind 0.4-μm aluminium shielding foil (a) and behind 0.15-μm aluminium shielding foil (c) in vacuum. Absolute values of supercoiled and relaxed DNA have been normalized to the control sample. (b),(d) Fits to the fractions of supercoiled DNA form vs photon fluences in the low-dose region. From the corresponding slopes of the fits, cross sections for SSBs creation were determined to be $(2.27 \pm 0.08) \times 10^{-17}$ m^2 and $(2.4 \pm 0.3) \times 10^{-17}$ m^2, respectively.

D. DNA damage quantification by agarose gel electrophoresis

The samples were analyzed to evaluate the fractions of supercoiled, linear, and relaxed plasmid forms by agarose gel electrophoresis. Irradiated and control samples containing about 110 ng DNA were mixed with 2 μl of 30% weight per volume (w/v) glycerol, 0.25% (w/v) xylene cyanol, 0.25% (w/v) bromophenol blue. The mixtures were applied to a neutral 0.8% agarose gels and run in 0.5X TAE buffer (20 mM Tris, 10 mM sodium acetate, 1 mM EDTA, pH 8.0) at 100 V. The gels were stained with SYBR Green I solution (1:10000, Sigma Aldrich, Taufkirchen, Germany). Images of the gels were taken on a UV transilluminator table (UVT-20ME; Herolab, Wiesloch, Germany) with an Olympus C-720 digital camera. Obtained images were transformed to black and white format and peaks corresponding to different forms of DNA were integrated by the homemade software LUTHIEN.

III. RESULTS AND DISCUSSION

A. Dependence of the yield of SSBs and DSBs on the CDL pulse fluence

Plasmid pBR322 DNA is a suitable system for studies of the biological action of XUV radiation on DNA at the molecular

level, which allows the measurement of both SSBs and DSBs within the same sample. Irradiation of the dried plasmid under vacuum with 26.5-eV XUV photons leads to further loss of the supercoiled DNA form and to the formation of the relaxed and the linear forms of the plasmid as a function of radiation dose.

Figures 3(a) and 3(c) show the yields of the different forms of DNA irradiated behind 0.4-μm and 0.15-μm Al foil, (i.e., the absorbed dose per one pulse was ~1.6 Gy/pulse and ~7.1 Gy/pulse, respectively). The yields, quantified in the gel, are plotted on the ordinate as the percentage of total amount of initial DNA as a function of photon fluence on the sample surface (the bottom axis), as well as a function of absorbed dose (the top axis). We observed that the quantity of surviving undamaged supercoiled DNA decreases with increasing XUV absorbed dose in a nonmonotonous way. The amount of relaxed DNA form increases with increasing photon fluence accordingly. This can testify to a contribution of the indirect effect caused by the XUV radiation. This finding is quite surprising because of a very low water content in the DNA material exposed in high vacuum. At large XUV exposures, the decrease in the supercoiled form of DNA is close to saturation, in the case of experiments with use of 0.4-μm Al foil, near 60% [Fig. 3(a)]. This suggests that no
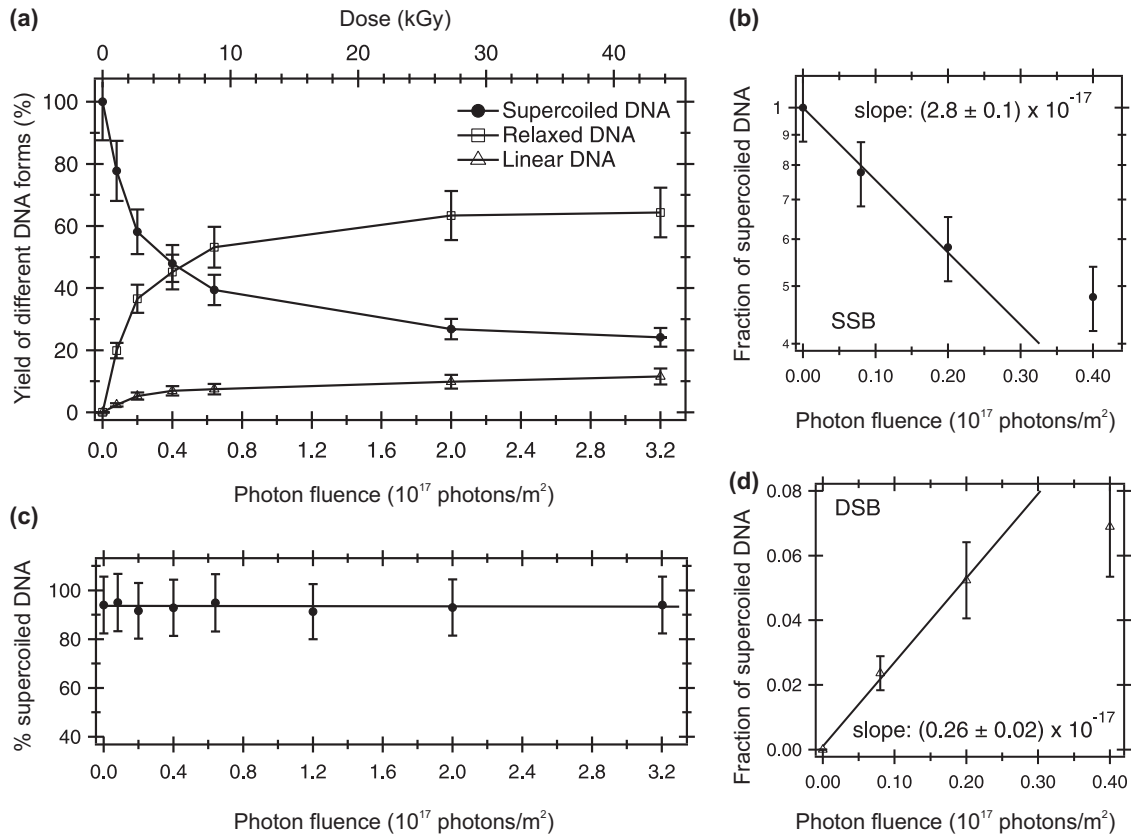
FIG. 4. Loss of supercoiled DNA and induction of SSBs and DSBs in plasmid DNA as a function of photon fluence on the sample surface (the bottom axis) and absorbed dose (the top axis) irradiated with 26.5-eV photons, without aluminium shielding foil (a), in a vacuum. Absolute values of supercoiled and relaxed DNA have been normalized to the control. The fit to the fraction of supercoiled DNA form vs photon fluence (b), as well as the fit to the fraction of linear DNA form vs photon fluence (d), in the low-dose region. (c) Yield of supercoiled DNA in plasmid DNA as a function of photon fluence irradiated behind LiF window. From the corresponding slope of the fits, cross sections for SSBs and DSBs creation were determined to be $(2.8 \pm 0.1) \times 10^{-17}$ m^2 and $(0.26 \pm 0.02) \times 10^{-17}$ m^2, respectively.

more than 40% of the plasmids in the solid can be converted to either relaxed or linear DNA. In the case of use of 0.15-μm Al foil the saturation in the decrease of supercoiled form of DNA occurs at 30% [Fig. 3(c)]. Prise *et al.* [11] observed a similar exponential loss of supercoiled DNA with the dose and a saturation from irradiation of DNA plasmids by low-energy photons. Considering the exponential dose response, i.e., assuming a Poisson-based decrease in undamaged targets, at high local levels of doses, further local dose increments cannot be efficiently transduced into measurable strand breaks, because multiple lesions on a target are not discriminated by the assay [31]. Furthermore, multiple SSBs are counted as one, and two or more well separated DSBs are not recorded at all. This can result in a saturation effect in lesion production [31].

The yield of different forms of DNA irradiated without using of the Al filters (the absorbed dose per one pulse ~11 Gy/pulse) is plotted in Fig. 4(a) analogously as in Fig. 3. We observed that the quantity of surviving undamaged super-coiled DNA decreases with increasing XUV photon fluence on the sample surface in a roughly exponential manner similarly as it was found in the previous case. At high absorbed doses, the decrease in supercoiled signal is close to saturation, near 20%.

Comparing the results in the figures, in the experiment with-out attenuated radiation from XUV laser we have observed,

unlike the irradiation behind Al foils at the same doses, the production of a linear form of the plasmid. The observed DNA SSBs damage presented in this paper can be assigned to 26.5-eV radiation exclusively due to the effective blocking of out-of-band radiation by aluminium foils. For unfiltered radiation as well the broadband incoherent UV-Vis radiation emitted from the plasma column of the capillary discharge is present. Effect of the broadband incoherent UV-Vis radiation exposure on plasmid DNA samples was studied by using a lithium fluoride window (<11.5 eV), filtering out 26.5-eV laser radiation. Figure 4(b) shows the loss of supercoiled DNA as a function of photon fluence for sample irradiated behind LiF window. At the same exposures as in the previous experiment, we did not observe significant effect of the broadband incoherent UV-Vis radiation on the plasmid DNA damage. DSBs were present probably due to the higher CDL pulse fluence, or due to the dual effect of 26.5-eV laser radiation and out-of-band radiation.

B. Effectiveness of the XUV photons in inducing DNA strand breaks

The initial responses in the low-dose region allowed us to estimate the damage yields [32]. At low doses, the yields of different forms of DNA are directly proportional to the
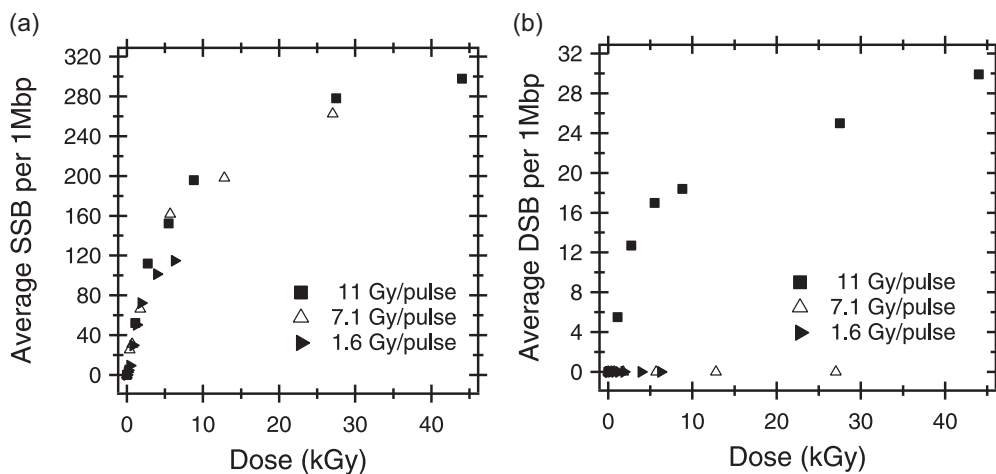
FIG. 5. Radiation chemical yields of (a) SSBs and (b) DSBs induced in pBR322 DNA plasmid induced by XUV laser.

action cross sections of the SSB and DSB induction. The fraction of SSBs as a function of the photon fluence was fitted by a least-squares method with an equation of the form $-\ln(S) = A \cdot F$, with S being the fraction of supercoiled DNA, A constant, and F corresponding to the photon fluence on the sample surface (photons/m^2) [33]. The slopes represent the action cross section of the SSBs, σ(SSB). The exponential dose-effect curve [Fig. 4(a)] indicates that a single-hit process was also obtained for DSBs induced by XUV photons; the fraction of DSB as a function of the photon fluence on the sample surface was fitted to a straight line by the least-squares methods. The slope represents the action cross section of the DSBs per photon fluence, σ(DSB). The cross section indicates the probability per XUV photon of inducing a DNA strand break in the pBR322 DNA plasmid molecule, thus reflecting the effectiveness of the XUV photons.

The cross sections for SSB induction in the case of all three experiments [i.e., behind 0.4-μm (1.6 Gy/pulse) and 0.15-μm Al foil (7.1 Gy/pulse) and without Al foil (11.0 Gy/pulse)] were calculated to be $(2.27 \pm 0.08) \times 10^{-17}$ m^2, $(2.4 \pm 0.3) \times 10^{-17}$ m^2 and $(2.8 \pm 0.1) \times 10^{-17}$ m^2, respectively. The fits are shown in Figs. 3(b), 3(d), and 4(c). The cross section for DSB induction was calculated to be $(0.26 \pm 0.02) \times 10^{-17}$ m^2. The fit is shown in Fig. 4(d). The cross section values for SSB induction are slightly increasing with increasing dose per pulse. Hieda *et al.* [7] measured cross sections for SSB induction in plasmids irradiated with 20.7-eV photons produced by a synchrotron radiation to be 1.6×10^{-17} m^2 and for DSB induction 0.02×10^{-17} m^2. Yokoya *et al.* [15] estimated cross sections of pBR322 plasmid DNA for single-strand-break induction to be 3.7×10^{-17} m^2, 3.9×10^{-17} m^2, and 5.2×10^{-17} m^2 for irradiation with ultrasoft x rays using monochromatic synchrotron radiation with energies 388, 435, and 573 eV, respectively. They found that cross sections of the strand breaks slightly increased with the photon energy. However, above-mentioned studies were done using the synchrotron radiation (SR) sources of energetic photons. Different time scales of CDL and SR radiation delivery should be taken into account and not only a difference in photon energies.

The radiation chemical yields of DNA SSBs and DSBs per plasmid molecule as a function of absorbed dose for all

three experiments (i.e., without Al foil and behind a particular Al filter) are presented in Figs. 5(a) and 5(b), respectively. The yields of SSBs and DSBs were determined from relative peak areas corresponding to the supercoiled (S), linear (L), and relaxed (R) forms of plasmid DNA separated on agarose gels. The yields of SSBs and DSBs were calculated as $G_{\text{SSB}} = \ln[(1 - L)/S]$ and $G_{\text{DSB}} = L/(1 - L)$, respectively, where $S + L + R = 1$ [34].

The G values (nmol J^{-1}), defined as the amount of substance (in moles) of SSBs and DSBs formed per joule of energy, absorbed in the plasmid DNA were calculated as $G = 1/[D_0/(MW)]$, where MW is the molecular weight of pBR322 DNA plasmid (2.86×10^6 daltons (Da)). Assuming Poisson distribution for strand-break induction [33], D_0 represents the radiation dose required to give, on average, one SSB or single hit DSB per plasmid molecule. The yields of SSBs and DSBs for 26.5-eV CDL radiation were determined to be 29.6 ± 3.2 and 3.1 ± 0.7 nmol J^{-1}, respectively. For comparison, Hieda *et al.* [7] found the value 25 nmol J^{-1} for 20.7-eV VUV photons. Brun *et al.* [35] estimated the G value for 1.5-keV x rays in vacuum to be 44 ± 6 nmol J^{-1}. So, there is a good agreement for the SSB formation.

The ratio of SSB and DSB yields was calculated to be $\sim$9.5 for 11 Gy/pulse (i.e., Al foil was not placed between the source and the sample). For 1-keV radiation, the ratio of SSB and DSB yields was determined to be 8.7 ± 0.8. The found value is close to the value of 8.7 in the study using single subnanosecond 1-keV x-ray pulse [17], 11 determined for 1.5-keV Al K_α x rays [36], and 10 obtained for γ radiation [37]. However, it could be misleading to generalize this agreement. It follows from Fig. 5(b) that the broadband UV-Vis emission of pinching capillary Ar discharge is likely enhancing XUV-initiated DSB formation. Such a synergic action of long- and short-wavelength radiations on polymer chain scissions has already been reported for synthetic organic polymers [38,39].

The finding can also be explained by a dose-rate effect in DSB formation. Strand breaks are formed by direct ionizations and excitations of DNA and low-energy electron interaction processes [12,20,35]. In addition, at high dose rates, the excitations of DNA cation radicals lead to the formation of sugar radicals that are precursors of strand breaks [40,41].

Therefore experiments using a stronger XUV-CDL source and applying more sensitive DSB analytical procedures are required to clarify this problem.

Among DBS formation mechanisms, the processes summarized in [42] are under our irradiation conditions more likely than processes assuming the participation of molecular oxygen in the damage, e.g., [43]. The high vacuum secures an absence of molecular oxygen in the sample.

To estimate a role of DNA hydration in the XUV radiolysis, we should keep in mind that the irradiation was performed in high vacuum. The Γ value (i.e., the number of water molecules per nucleotide) in the vacuum is considered to be $\Gamma = 2.5$ [44]. In such a low hydration of the DNA, the hole transfer dominates over an action of OH radicals as has been shown by Purkayastha *et al.* [45] for γ radiation and x rays. Strand breaks in the weakly hydrated DNA exposed to XUV radiation at high doses (11.0 Gy/pulse) are likely caused by deoxyribose-sugar radicals formation [40].

After XUV exposure in the vacuum, we found strand-break yields related to the values determined by Purkayastha *et al.* [46] in almost fully hydrated DNA ($\Gamma > 22.5$). More experiments on wider linear energy transfer (LET) LET/Γ

variety are needed to make a conclusion about mechanisms behind these relations.

IV. CONCLUSIONS

Both SSB and DSB yields were determined in plasmid DNA irradiated by nanosecond pulses of 46.9-nm laser radiation. Obtained values of SSB yields clearly indicate that XUV CDL initiated chemical changes in DNA are more similar to that caused by an ionizing radiation rather than photomodification due to ultraviolet illumination. We observed an increase in the efficiency of induction of strand breaks in supercoiled DNA as a function of laser pulse fluence. In conclusion, XUV CDL has been proven as a source of ionizing electromagnetic radiation which is suitable for investigation of radiation damage to biomolecular solids.

ACKNOWLEDGMENTS

[1] C. Von Sonntag, Int. J. Radiat. Biol. **66**, 485 (1994).

[2] K. Tasak, X. Yang, S. Urano, S. Fetzer, and P. R. LeBreton, J. Am. Chem. Soc. **112**, 538 (1990).

[3] D. Roca-Sanjuán, M. Rubio, M. Merchán, and L. Serrano-Andrés, J. Chem. Phys. **125**, 084302 (2006).

[4] T. Inagaki, J. Chem. Phys. **61**, 4246 (1974).

[5] W. Sontag and K. F. Weigezahn, Radiat. Environ. Biophys. **12**, 169 (1975).

[6] T. Douki, T. Zalizniak, and J. Cadet, Photochem. Photobiol. **66**, 171 (1997).

[7] K. Hieda, Int. J. Radiat. Biol. **66**, 561 (1994).

[8] G. Vall-Llosera, M. A. Huels, M. Coreno, A. Kivimäki, K. Jakubowska, M. Stankiewicz, and E. Rachlew, Chem. Phys. Chem. **9**, 1020 (2008).

[9] T. Ito and M. Saito, Radiat. Phys. Chem. **37**, 681 (1991).

[10] A. Mozumder, Phys. Chem. Chem. Phys. **4**, 1451 (2002).

[11] K. Prise, M. Folkard, B. Michael, B. Vojnovic, B. Brocklehurst, A. Hopkirk, and I. Munro, Int. J. Radiat. Biol. **76**, 881 (2000).

[12] B. Boudaïffa, P. Cloutier, D. Hunting, M. A. Huels, and L. Sanche, Science **287**, 1658 (2000).

[13] M. Folkard, K. M. Prise, B. Brocklehurst, and B. D. Michael, J. Phys. B **32**, 2753 (1999).

[14] B. Zielbauer, J. Habib, S. Kazamias, O. Guilbaud, M. Pittman, D. Ros, M. A. H. du Penhoat, A. Touati, C. Le Sech, E. Porcel, and S. Lacombe, *X-Ray Lasers 2008*, Springer Proceedings in Physics, edited by C. L. S. Lewis and D. Riley (Springer Netherlands, Belfast, 2009), Vol. 130, pp. 409–411.

[15] A. Yokoya, R. Watanabe, and T. Hara, J. Radiat. Res. **40**, 145 (1999).

[16] B. Fayard, A. Touati, E. Sage, F. Abel, C. Champion, and A. Chetoui, J. Chim. Phys. Phys.-Chim. Biol. **96**, 147 (1999).

[17] M. Davídková, L. Juha, M. Bittner, S. Koptyaev, V. Hájková, J. Krása, M. Pfeifer, V. Štísová, A. Bartnik, H. Fiedorowicz, J. Mikolajczyk, L. Ryc, L. Pína, M. Horváth, D. Babánková, J. Cihelka, and S. Civiš, Radiat. Res. **168**, 382 (2007).

[18] A. Eschenbrenner, M.-A. Herve Du Penhoat, A. Boissiere, G. Eot-Houllier, F. Abel, M.-F. Politis, A. Touati, E. Sage, and A. Chetioui, Int. J. Radiat. Biol. **83**, 687 (2007).

[19] A. Yokoya, S. M. T. Cunniffe, R. Watanabe, K. Kobayashi, and P. O'Neill, Radiat. Res. **172**, 296 (2009).

[20] E. Alizadeh, P. Cloutier, D. Hunting, and L. Sanche, J. Phys. Chem. B **115**, 4523 (2011).

[21] S. Heinbuch, M. Grisham, D. Martz, and J. J. Rocca, Opt. Express **13**, 4050 (2005).

[22] J. J. Rocca, V. Shlyaptsev, F. G. Tomasel, O. D. Cortazar, D. Hartshorn, and J. L. A. Chilla, Phys. Rev. Lett. **73**, 2192 (1994).

[23] S. G. Swarts, M. D. Sevilla, D. Becker, C. J. Tokar, and K. T. Wheeler, Radiat. Res. **129**, 333 (1992).

[24] R. E. Franklin and R. G. Gosling, Nature (London) **172**, 156 (1953).

[25] L. Vyšín, T. Burian, J. Chalupský, M. Grisham, V. Hájková, S. Heinbuch, K. Jakubczak, D. Martz, T. Mocek, P. Pira, J. Polan, J. J. Rocca, B. Rus, J. Sobota, and L. Juha, in *Damage to VUV, EUV, and X-Ray Optics II*, edited by L. Juha, S. Bajt, and R. Sobierajski (SPIE, Bellingham, WA, 2009), Vol. 7361, pp. 73610O–73610O–8.

[26] E. Nováková, M. Davídková, L. Vyšín, T. Burian, M. E. Grisham, S. Heinbuch, J. J. Rocca, and L. Juha, in *Damage to VUV, EUV, and X-Ray Optics III*, edited by L. Juha, S. Bajt, and R. A. London (SPIE, Bellingham, WA, 2011), Vol. 8077, pp. 80770W–80770W–8.

[27] L. Urbanski, M. C. Marconi, L. M. Meng, M. Berrill, O. Guilbaud, A. Klisnick, and J. J. Rocca, Phys. Rev. A **85**, 033837 (2012).

[28] G. D. Fasman, *Handbook of Biochemistry and Molecular Biology*, 3rd ed. (CRC, Cleveland, 1989), p. 616.

[29] J. G. Sutcliffe, Cold Spring Harbor Symposia on Quantitative Biology **43**, 77 (1979).

[30] B. Henke, E. Gullikson, and J. Davis, At. Data Nucl. Data Tables **55**, 349 (1993).

[31] G. Taucher-Scholz and G. Kraft, Radiat. Res. **151**, 595 (1999).

[32] B. Michael, K. Prise, M. Folkard, B. Vojnovic, B. Brocklehurst, I. Munro, and A. Hopkirk, Int. J. Radiat. Biol. **66**, 569 (1994).

[33] L. F. Povirk, W. Wübker, W. Köhnlein, and F. Hutchinson, Nucleic Acids Res. **4**, 3573 (1977).

[34] K. Hempel and E. Mildenberger, Int. J. Radiat. Biol. **52**, 125 (1987).

[35] E. Brun, P. Cloutier, C. Sicard-Roselli, M. Fromm, and L. Sanche, J. Phys. Chem. B **113**, 10008 (2009).

[36] Z. Cai, P. Cloutier, L. Sanche, and D. Hunting, Radiat. Res. **164**, 173 (2005).

[37] A. Yokoya, S. M. T. Cunniffe, and P. O'Neill, J. Am. Chem. Soc. **124**, 8859 (2002).

[38] T. Mocek, J. Polan, P. Homer, K. Jakubczak, B. Rus, I. J. Kim, C. M. Kim, G. H. Lee, C. H. Nam, V. Hájková, J. Chalupský, and L. Juha, J. Appl. Phys. **105**, 026105 (2009).

[39] F. Barkusky, C. Peth, A. Bayer, and K. Mann, J. Appl. Phys. **101**, 124908 (2007).

[40] A. Adhikary, S. Collins, D. Khanduri, and M. D. Sevilla, J. Phys. Chem. B **111**, 7415 (2007).

[41] D. Khanduri, A. Adhikary, and M. D. Sevilla, J. Am. Chem. Soc. **133**, 4527 (2011).

[42] A. Adhikary, D. Becker, and M. D. Sevilla, in *Applications of EPR in Radiation Research*, edited by A. Lund and M. Shiotani (Springer, Berlin, Heidelberg, 2014), Chap. 8, pp. 299–352.

[43] M. L. Taverna Porro and M. M. Greenberg, J. Am. Chem. Soc. **135**, 16368 (2013).

[44] N. J. Tao, S. M. Lindsay, and A. Rupprecht, Biopolymers **28**, 1019 (1989).

[45] S. Purkayastha, J. R. Milligan, and W. A. Bernhard, Radiat. Res. **166**, 1 (2006).

[46] S. Purkayastha, J. R. Milligan, and W. A. Bernhard, J. Phys. Chem. B **110**, 26286 (2006).